μPIV MEASUREMENT AND NUMERICAL COMPUTATION OF THE VELOCITY PROFILES IN MICROCHANNELS

Cătalin Mihai BĂLAN[1], Corneliu BĂLAN[2]

Lucrarea de faţă prezintă rezultatele obţinute în urma studiilor numerice şi experimentale dedicate măsurării şi modelării profilurilor de viteze în micro-canale, atât pentru fluide pur vâscoase newtoniene cât şi pentru fluidele complexe ce prezintă un caracter pseudoplastic. Cinematica mişcărilor studiate în micro-bifurcaţii tip Y este determinată cu ajutorul unui sistem micro-PIV, simulările corespunzătoare fiind realizate cu ajutorul codului FLUENT. Soluţiile numerice în configuraţii 3D, confirmate calitativ şi cantitativ de măsurătorile experimentale, permit extinderea studiului în aplicaţii specifice micro-fluidicii: amestecul fluidelor imiscibile, analiza fenomenului de difuzie, transportul fluidelor bifazice.

The present paper is dedicated to the experimental investigations and numerical simulations of the velocity distributions in micro-channels geometry, for pure viscous Newtonian fluids and complex fluids characterized by the shear thinning behavior. The steady flow kinematics in Y-micro-bifurcation is determined with a micro-PIV measurement system, the simulations being performed with the FLUENT commercial code. Numerical solutions obtained in 3D configurations, validated from qualitative and quantitative by experiments, can be extended to more complex specific micro-fluidics applications: mixing of immiscible fluids, analysis of diffusion process, transport of biphasic fluids.

Keywords: Micro-fluidics, channel flow, **v**elocity profiles, μPIV, Complex fluids

1. Introduction

In the last decade, micro-fluidic devices have emerged as a powerful toolset for miniaturization and automation of fluid handling and fluid analysis, [1]. The numerous advantages of micro-fluidics: the reduced amounts of sample and reagents needed, the high surface to volume ratio, the substantial waste reduction, the low cost of fabrication and the possibility of producing highly integrated and disposable devices, have stimulated a large scientific interest and generated extensive range of applications in advanced and novel areas of engineering that include: propulsion and power generation of micro-satellites, micro air vehicles, inkjet printer heads, and bio analytical instruments.

[1] PhD student, , Hydraulics, Fluid Machinery and Envioremental Engineering Department, University POLITEHNICA of Bucharest, Romania
[2] Prof., , Hydraulics, Fluid Machinery and Envioremental Engineering Department, University POLITEHNICA of Bucharest, Romania, e-mail: corneliu.balan@upb.ro

The micro-fluidic flows are characterized by small length-scales, high deformation rates and small Reynolds numbers, even thought the characteristic viscosity has the same order of magnitude with water. In almost all the applications the samples are complex fluids with a very sensitive rheology to their formulation, [2], [3]. The micro-devices are typically composed of a series of planar channels involving either sudden changes in direction (T or Y sharp shapes, serpentines of the channels walls), [4], or abrupt variation of the flow area (contraction or extension), [5]. For this reason, the modeling of fluid dynamics in those prototypical configurations, such as the planar configuration of T or Y shapes, is of utmost importance for developing particular applications.

The main goal of the present paper is to evidence, using experimental and numerical investigations, the differences that appear in the velocity profiles of non-Newtonian fluids transported in micro-channels, in comparison to the pure viscous fluid. This subject of study represents a benchmark problem in micro-fluidics and a test of the numerical procedure used to model such flows.

2. Experimental methodology

The geometry used in this work is a Y-symmetrical micro-bifurcation from plexiglas. The cross-sectional area is a square ($h = w_c = 700\ \mu m$) with the angle $\theta = 75°$ between the branches E_2 and E_3, see Fig. 1.

The lengths of the upstream and downstream branches are long enough so the flow in vicinity of bifurcation is not influenced by the "end effects". The present investigations are focused in *Zone A* that appears market in Fig. 1.b, flow area with fully developed stable velocity profile. A controlled displacement-rate syringe pump was used to impose a constant flow rate Q, $27 \leq Q \leq 254\ ml \cdot h^{-1}$. The steady flow kinematics is visualized and measured using a shadow streak imaging procedure and the micro-particle image velocimetry (μPIV), [6], [7]. The working set-up is presented in Fig. 2.

The μPIV technique determines the velocity distribution using a double frame imaging technique, with a cross-correlation algorithm for extracting the local particle displacements during the time gap between the two consecutive frames (the fluid was previously seeded with 0.9 μm diameter particles at a weight concentration of 0.02%). A CCD camera (Dantec 80C77 Hisense; 1280x1024 pixels) with an adjustable exposure time (depending on flow conditions and the focusing region in order to satisfy the algorithm constraints) was used to acquire the images. This camera was connected to a classical microscope using a 4X magnification objective (M) with a numerical aperture of $NA = 0.1$.

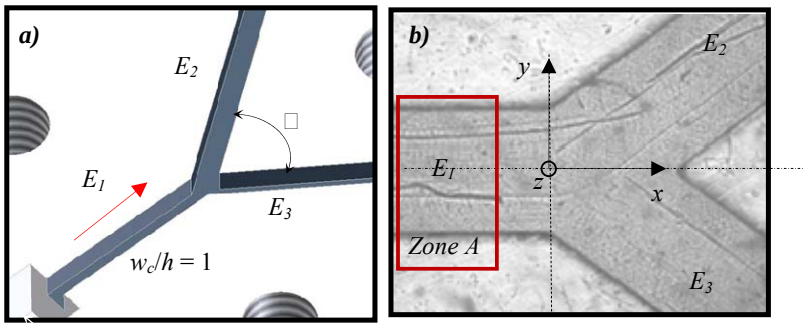

Fig. 1. Geometric characteristics of the micro-channel. ***a)*** Schematic diagram of the planar microgeometry. ***b)*** Optical transmission microscope image with 4X magnification (center plan).

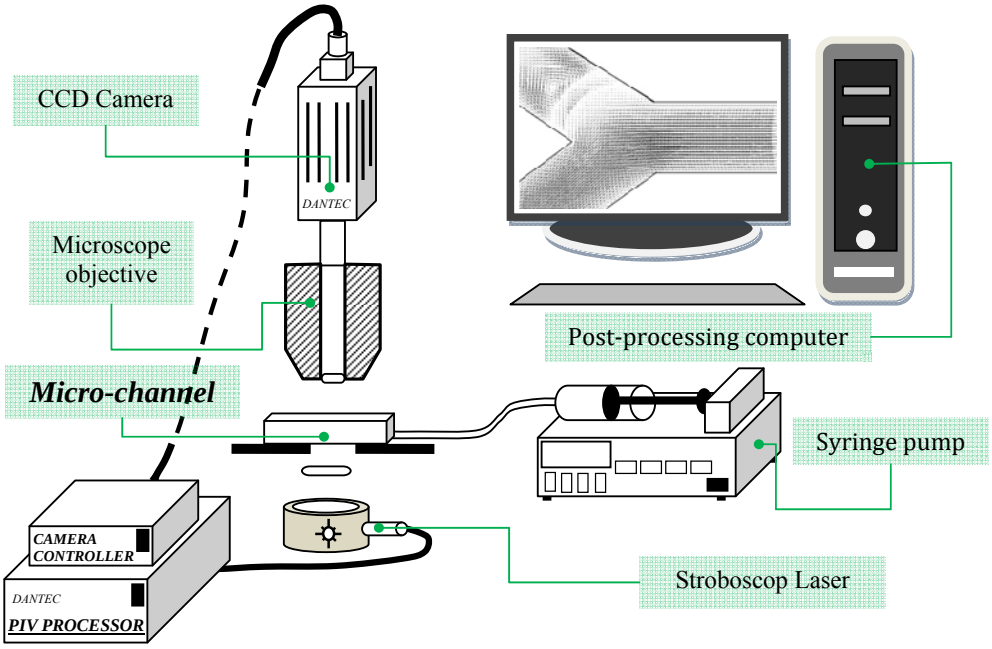

Fig. 2. Schematic representation of the μPIV measuring system.

Because the micro-device is made from plexiglas it was able to illuminate the flow from below with a stroboscope laser light. The depth of measurement corresponds to a band of 182 μm, which represent up to 26% of the channel depth in the observable streak line images. The thickness of that band defines the set-up precision in location (within the height of the channel) of the measured velocity profile. For all cases, a minimum of 20 image pairs were recorded, divided into interrogation areas of 32x32 pixels. These images were processed and averaged

ensemble using the software package ImageManager (version 4.71) delivered by Dantec. For processing the images it was used a Nyquist algorithm with a 50% overlap to generate the 2D velocity vector maps.

The visualizations and measurements were performed using Newtonian liquids (water and solutions of glycerin in water) and weekly-elastic fluids solutions, water solutions of ***p***oly***a***cryl***a***mide (PAA) with a molecular weight of 18M, [9]. Polyacrylamide solutions are viscoelastic fluids with a relevant shear-thinning behavior. The dynamic viscosities of the samples with 500 ppm and 1000 ppm concentration are shown in Fig. 3. The measurements were performed in a cone and plate configuration using a PHYSICA MCR 301 rheometer. The existence of two Newtonian plateaus (η_0 and η_∞) suggests the possibility of applying the Carreau-Yasuda model for fitting viscosity from Fig. 3,

$$\eta = \eta_\infty + \frac{\eta_0 - \eta_\infty}{\left(1 + (\lambda\dot{\gamma})^a\right)^{\frac{1-n}{a}}} \,. \tag{1}$$

where three more parameters are involved: λ – is the specific time; a – parameter defining the broadness of the interval over which the viscosity function decreases; n – coefficient determining the slope of the viscosity curve, see Tab. 1.

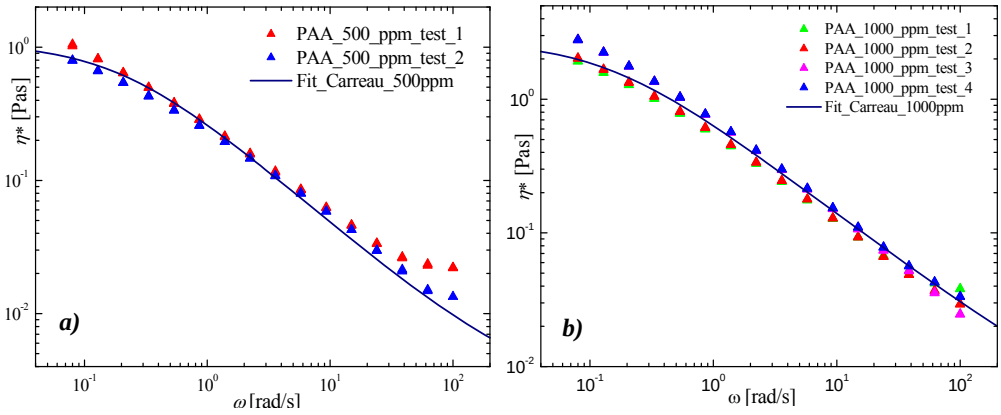

Fig. 3. The rheological results: ***a)*** polyacrylamide 500 ppm ***b)*** polyacrylamide 1000 ppm.

Table 1

Carreau Yasuda model – characteristic material parameters at 21° C

Name	Concentration	η_o [$Pa{\cdot}s$]	η_∞ [$Pa{\cdot}s$]	λ [s]	n [-]	a [-]
PAA 500	500 ppm	1.08	0.0023	5	0.2	1
PAA 1000	1000 ppm	2.7	0.00315	7	0.2	1

3. Numerical procedure

In addition to the experimental measurements ,there were performed several 3D calculations to simulate the isothermal flow of the viscous and shear thinning fluids through the microgeometry in the zone of interest (see Fig. 1).The simulations are performed with FLUENT™ CFD package, laminar steady solver (double precision) with convergence criteria of 10^{-10}. The code solves the Cauchy equation of motion, for incompressible fluids – $tr\mathbf{D} = 0$, in which the extra-stress tensor is expressed as a generalized Newtonian model:

$$\rho\left[\frac{\partial \mathrm{u}}{\partial t} + (\mathrm{u}\nabla)\mathrm{u}\right] = \rho\boldsymbol{b} - \nabla p + 2\nabla(\eta(\dot{\gamma})\mathrm{D}) \tag{2}$$

where ρ is the fluid density (assumed constant), $\boldsymbol{b}$ is the unitary mass force, **D** is the stretching, **u** the velocity vector, p the pressure and $\eta(\dot{\gamma})$ the viscosity function, dependent on shear rate (for a Newtonian fluid $\eta(\dot{\gamma}) = \eta_0$ = constant).

The validity of the continuum hypothesis and the no-slip boundary condition were assumed also for all tested fluids, [5]. A block-structured orthogonal non-uniform mesh is used to map the computational 3D domain; the total number of cells mesh is NC = 910.000. The characteristic Reynolds number of the Newtonian flows is defined as $Re = \dfrac{4\rho U R_h}{\eta_0}$, where the hydraulic radius $R_h = h \cdot w_c / 2(h+w_c)$ and the average velocity $U = Q/h \cdot w_c$ are used, [10].

4. Results and discussion

The velocity distribution is measured using the μPIV system and compared with the corresponding numerical results in the center plan ($z = 0$) from *Zone A*, see Fig. 1. The first validation of the experiments is the comparison of the measured velocity profiles at $z = 0$ with the corresponding analytical 2D solution for a Newtonian fluid, see Fig. 4. The agreement between the two velocity profiles is very good, with the exception of the region very near by the wall, where the resolution and precision of the measurements is low. The results also validate the assumption that velocity profile in the test region is un-perturbed and in the center plan the motion has a 2D structure.

The experimental and numerical velocity profiles in tested section, at different flow rates, are represented for some tested fluids in Fig. 5 and Fig. 6 ($27 \leq Q \leq 254$ $ml \cdot h^{-1}$, that correspond to Re numbers between 10 and 90 for water). As was expected, the prediction of velocity distributions for Newtonian fluids is very good, see Fig. 5. Even if Carreau-Yasuda model (Tab. 1) used in simulations does not contain elasticity, the computed velocities corresponding to the polymer solutions are in a good agreement with the measurements, see Fig. 6.

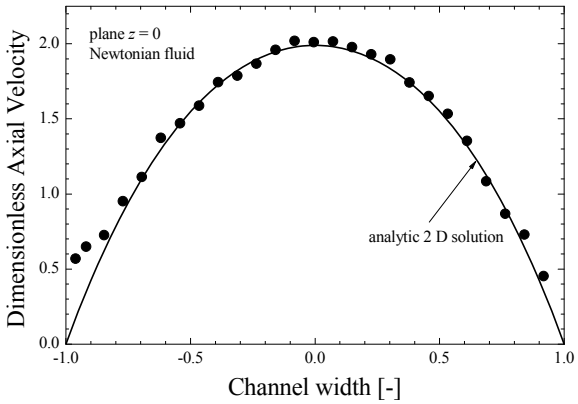

Fig. 4. Comparison of the velocity profiles determined experimentally (symbols) at a constant flow rate $Q = 27\ ml \cdot h^{-1}$ ($Re = 10$) and the analytical solutions (solid line) for Newtonian flow, [11].

It is evident from the experimental results that velocity profiles become more spread at higher flow rates. For smaller flow rates, the algorithm of generating the 2D velocity vector maps is using images divided into interrogation areas of 32x32 pixels, but when the flow rate is increased the velocity profiles can be obtained only if the images are divided in interrogations area of normally 64x64 pixels. This has an important effect on the number of measured velocity vectors which define at the end the 2D velocity profiles. Therefore, one concludes that a good qualitative and quantitative agreement between computation and measurements is obtained for $Re < 50$.

5. Conclusions

This study performed detailed investigations of the modeling of Newtonian and non-Newtonian steady flows in a 3D micro-geometry containing symmetrical micro-bifurcation. The central goal of the work is to validate the numerical procedure for the 3D representation of fully developed velocity profiles of generalized Newtonian flows micro-channels. The investigations were carried out from both experimental and numerical perspectives, the corresponding results being founded in very good agreement, up to $Re = 50$.

The μPIV technique allowed accurate measurements of the velocity field for a relatively large range of flow rates ($27 \leq Q \leq 254\ ml \cdot h^{-1}$). Numerical simulations and experiments are found consistent for different liquids, see Fig. 7, which is an indication that numerical code can be successfully extended to more complicated micro-geometries. The investigations and modeling of micro-vortical structures is the next target of our studies.

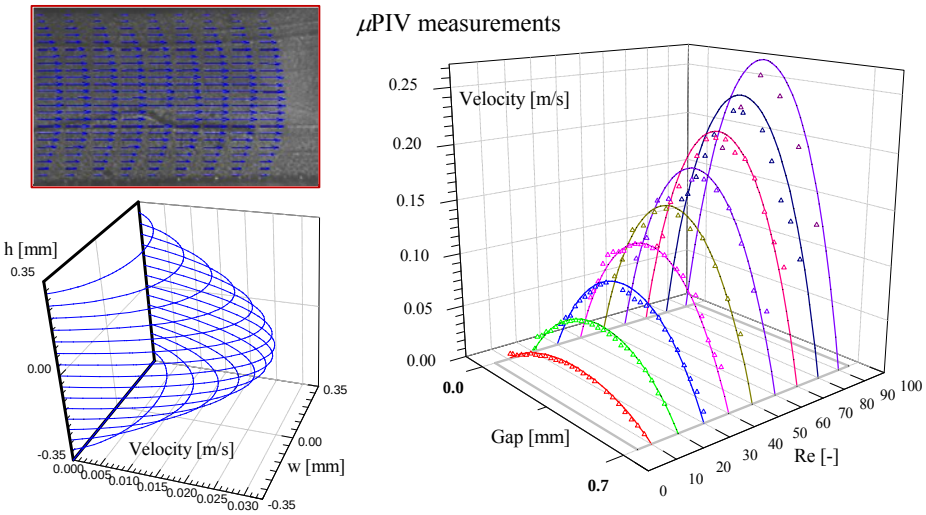

Fig. 5. Experimental velocity distribution (open symbols Δ) obtained with the μPIV system, compared with the numerical predictions (continues lines —) for water.

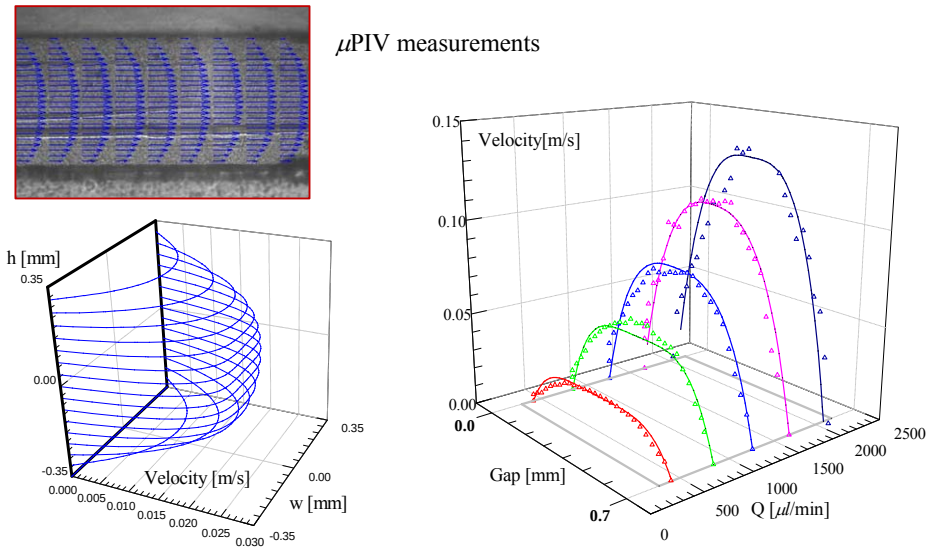

Fig. 6. Experimental velocity distribution (open symbols Δ) obtained with the μPIV system, compared with the numerical predictions (continues lines —). The working fluid is polyacrylamide with a concentration of 1000 ppm, respectively Carreau-Yasuda model.

One conclude that ability of the 3D numerical calculations to accurately capture both the kinematics and dynamics observed experimentally provides a procedure at hand for rapidly exploring the hydrodynamics associated to micro-fluidic devices and their applications.

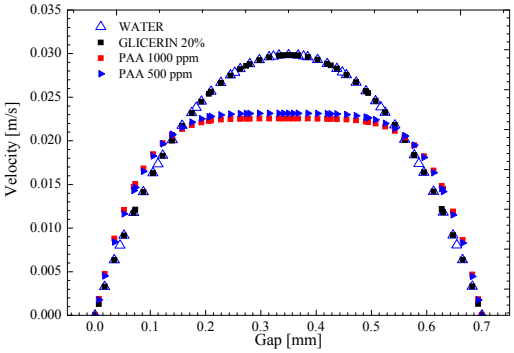

Fig. 7. Numerical velocity profiles for different fluids ($Q = 27\ ml \cdot h^{-1}$).

Acknowledgements

The Ph.D. Student Catalin Mihai Balan, acknowledges the financial support of the *CNCSIS grant BD 73*.

R E F E R E N C E S

[1]. *G. M .Whitesides,* "The origins and the future of microfluidics", Nature, **vol. 442**, 2006, pp. 368-373

[2]. *H. A. Stone, A. D. Stroock and A. Ajdari*, "Engineering flows in small devices: Microfluidics toward a Lab-on-a-Chip", A. Rev. Fluid Mech., **vol. 36**, 2004, pp. 381-411

[3]. *T. M. Squires and S. R. Quake*, "Microfluidics: Fluid physics at the nanoliter scale", Rev. Modern Physics, **vol. 77**, 2005, pp. 977-1026

[4]. *A. E. Kamholz, B. H. Weigl, B. A. Finlayson and P. Yager*, "Quantitative analysis of molecular interaction in a microfluidic channel: T-sensor", Anal. Chem., **vol. 71**, 1999, pp. 5340-5347

[5].*M. S. N. Oliveira, L. E. Rodd, G. H. McKinley and M. A. Alves*, "Simulations of extensional flow in microrheometric devices", J. Microfluid Nanofluid, **vol. 5**, 2008, pp. 809-826

[6]. *J. G. Santiago, S. T. Wereley, C. D. Meinhart, D. J. Beebe and R. J. Adrian,* "Particle image velocimetry systems for microfludics", Exp. Fluids, **vol. 25**, pp. 316–319

[7].*S. T. Wereley and C. D. Meinhart*, Micron-resolution particle image velocimetry, in: Breuer KS (ed.) Microscale diagnostic techniques, Springer, Berlin, 2004

[8].*M. S. N. Oliveira, M. A. Alves, F. T. Pinho and G. H. McKinley*, "Viscous flow through microfabricated hyperbolic contractions", Exp. Fluids, **vol. 43**, 2007, pp. 437–451

[9].*Andreea Calin,* Modeling the flow of polymeric fluids in complex geometries, Ph.D. Thesis, University Politehnica of Bucharest, 2008

[10]. *M. Gad-el-Hak*, The MEMS handbook. CRC Press, Boca Raton, 2002

[11]. *H. Bruus*, Theoretical microfluidics, Oxford Univ. Press, 2008.